Results in Engineering 17 (2023) 100850

Contents lists available at ScienceDirect

Results in Engineering

journal homepage: www.sciencedirect.com/journal/results-in-engineering

Research Paper

A meta-heuristic optimization-based method for parameter estimation of an electric arc furnace model

J.J. Marulanda-Durango [a,*], C.D. Zuluaga-Ríos [b]

[a] Electrical Engineering Program, Universidad Tecnológica de Pereira, Pereira, Colombia
[b] Department of Electrical Engineering, Institución Universitaria Pascual Bravo, Medellín, Colombia

ARTICLE INFO

Keywords:
Parameter estimation
Ac electric arc furnaces
Power quality problems
Meta-heuristic optimization

ABSTRACT

Throughout distribution systems, it is usual to find non-linear time-varying loads, such as electric arc furnaces (EAFs), which are widely used in the steel-making industrial sector. Due to the process of melting and refining metals, the EAFs consume large blocks of power (active and reactive power) causing significant power quality disturbances, such as harmonics and voltage fluctuations on distribution networks. Different EAF parametric models have been proposed with the purpose to predict the voltage and current waveforms and then evaluate the performance of the reactive power compensation devices. This paper proposes a novel methodology for the optimal estimation of parameters of an electric arc furnace model, which can achieve lower execution times and error rates compared to some state-of-the-art methods. The methodology was evaluated using three meta-heuristic optimization algorithms such as the particle swarm optimization (PSO) algorithm, the vortex search algorithm (VSA) and the crow search algorithm (CSA); using real and simulated data. From the results, the proposed methodology based on meta-heuristic optimization approaches worked efficiently, allowed estimating the parameters of the electric arc furnace model using a single optimization step, capture the non-sinusoidal, non-linearity and time-varying random behavior that exhibit the real electric arc furnace samples and obtained relative errors of the total harmonic distortion between the measured and estimated voltage and arc current signals around 1.23% and 0.62%, respectively.

1. Introduction

The EAFs are one of the largest loads for the electrical power system, they are used for producing aluminium, copper, high-quality steel, among other metals [1]. However, they are considered important threats to the power quality (PQ), because their operation generates harmonics and interharmonics, voltage flickers, and unbalances in the voltages and currents at the point of common coupling [2]. The non-linear voltage-current characteristic of the electric arc, the irrand regularities in the shape of the metal to be melted, and the constant triggering of the electric arc during the melting process, cause low PQ indexes [3]. Electric utilities and industrial facilities that have an EAF, make significant efforts to implement technical and economical solutions to mitigate the PQ problems associated with the EAF operation [4]. Solutions include the use of mathematical models of the EAF which can be used in electrical circuit simulation programs, for evaluating the adverse effects generated by the EAF in existing plants, or in new facilities considering data from similar installations. Likewise, the electric arc models are also used to assess the performance of different compensating devices such as SVC, synchronous static var compensator (STATCOM), active power filters (APF), and –still under study– energy storage systems (ESS) [5].

The electric arc model is a valuable computation tool to obtain the electric response of an EAF. Different mathematical models have been proposed in the literature to capture the physical responses associated with the dynamics of the electric arc model. For example, a linear model based on linear electrical circuit elements and a current source has been proposed in [3,5]. The authors in [6,7] considered a time-variant non-linear resistance to model the electric arc. Electric arc models based on parametric equations are presented in [8–11]. Models based on chaotic systems are used [12–15] to generate the chaotic variations in the time response of the EAF. Other models consider a stochastic signal to capture the arc length variations [8,16]. Data-driven learning models are presented in [2,17–23].

Although several approaches have been proposed to capture the dynamics of the EAF model, few methodologies have focused on esti-

* Corresponding author.
E-mail addresses: jjmarulanda@utp.edu.co (J.J. Marulanda-Durango), carlos.zuluaga@pascualbravo.edu.co (C.D. Zuluaga-Ríos).

https://doi.org/10.1016/j.rineng.2022.100850
Received 27 October 2022; Received in revised form 13 December 2022; Accepted 13 December 2022
Available online 20 December 2022

mating the parameters of this model. Specifically, these methodologies seek to calibrate the model parameters through a procedure in which the outputs of the model are adjusted using observed data, by varying the values of the parameters of the model [24]. These approaches can be classified into three main groups: simulation-based methods [1,6], data-driven techniques [25,26] and methodologies based on optimization problems [27,7,28,11]. In [1], the range of variation of the arc resistance is determined using a static curve that relates the active power of the arc furnace to the power factor. A calibration method based on trial and error is proposed in [6]. The method is stopped when a difference between the simulated and measured active power less than 1% is obtained. The drawback of this method is that the simulated voltages and currents generated from the model may differ from the corresponding real measurements [6]. The second group includes approaches such as the least-mean square method or support vector machines (SVMs). For example, in [25] the authors presented a linear model based on the transformation of the Mayr and Cassie models, and by using the least-mean square method (LSM) to adjust the equivalent regression model with real data. Nonetheless, this method presents difficulties in the dynamic representation of the EAF model. In addition, the authors in [26] proposed a data-driven approach to identify a non-linear time-varying chaotic model, considering multi-input multi-output SVMs. This method considers the use of excessive data generated through simulations from the model to train the SVMs. In the last group are methods based on linear programming [27], genetic algorithms [7,28] and differential evolution algorithm [11] to determine the parameters of the EAF model. In the last two optimization methods, despite obtaining near-optimal solutions, neither gradients nor Hessians are used to calculate the optimal solutions. However, the methods presented in [7,28] divide the parameters of the electric arc model into deterministic and stochastic, in which each set of parameters (i.e. deterministic and stochastic) is identified by minimizing a different objective function. These approaches increase the execution time to determine the parameters of the electric arc model. The disadvantage of the method proposed in [11] is the fact that the behavior of arc-length is assumed to be deterministic, which is far from real experiments.

This paper addresses these shortcomings by formulating the electric arc model parameter estimation problem as a novel methodology based on the minimization of a single-objective function, different to the methodologies proposed by [7] and [28]. Additionally, this methodology allows capturing the non-sinusoidal, non-linearity and time-varying random behavior that exhibits the real electric arc furnace samples. The estimation has been carried out in each half cycle of the real measurements, to take into account the arc reignition in each half cycle, and the variations that exhibit the reactive power consumed by the furnace, which is required when the model is used to evaluate the performance of flicker mitigation devices [25].

From this methodology, six optimization approaches have been applied to estimate the parameters of this system. Three of them have been reported within the state of the art and the rest are proposed as alternative solution methodologies. Specifically, this paper proposes the use of the particle swarm optimization (PSO) algorithm, the vortex search algorithm (VSA) and the crow search algorithm (CSA), which have not been considered yet in the literature, to estimate the parameters of an EAF system. The main reasons to select these algorithms are the following: the PSO is the most popular algorithm of swarm intelligence methods, which consists of a population of particles, known as a swarm, with each member of the swarm being associated with a position and a velocity. These terms are updated by using stochastic weights, previous positions and velocity rules. The VSA is easy to implement and proposes good candidate solutions for real optimization problems. The VSA is a natural phenomena approach that is inspired by the vortex pattern created by the vortical flow of the stirred fluids. This algorithm proposes new candidate solutions from a Gaussian distribution by using the current best solution at each iteration. The VSA uses an inverse incomplete gamma function to decrease the value of the radius (the variance of the Gaussian distribution) during each iteration. On the other hand, the CSA is another population intelligence technique that is easy to implement, depends on a few parameters and has flexibility. The CSA is based on the intelligent behavior of crows, that is, the algorithm follows the idea that crows store their excess food in safe places and get it back when they need it. The main contributions of this paper include the following:

- A novel methodology based on the minimization of a single-objective function for estimating the EAF model parameters is introduced. According to the results obtained, this methodology allows capturing the non-sinusoidal, non-linearity and time-varying random behavior that exhibits the real electric arc furnace samples, during the melting phase of the furnace operation.
- Five of the most commonly used meta-heuristic algorithms have been considered in the optimization problem, to estimate the parameters of the EAF model.
- A detailed comparative analysis of the considered meta-heuristic algorithms is presented. Real data have been used to evaluate the performance of the proposed method. In addition, a method based on least squares has been considered to evaluate its computational cost and accuracy concerning the meta-heuristic algorithms.

This paper is organized as follows: Section 2 presents a short description of the non-linear dynamic EAF model. Section 3 describes the proposed method to estimate the parameters of the electric arc model. Simulation results are presented in Section 4, and the conclusions are given in Section 5.

2. Electrical power supply system and model of the electric arc

The EAF used in this study is feeder by an electrical power circuit whose single-phase circuit diagram is shown in Fig. 1. The main components of the circuit are: the utility grid which is modeled per phase by an electrical voltage source v_s in series with an inductor L_s, the high voltage (HV)-medium voltage (MV) transformer T_1 with Y-Δ connection, the MV-low voltage (LV) transformer T_2 with $\Delta-\Delta$ connection, and the flexible cooled cables which connect the LV side of the transformer T_2 with the electrodes, represented in the circuit by the resistor R_c in series with the inductor L_c. The actual voltage and current data used in this work were taken from the real installation described in [26]. Therefore, the values of the circuit elements shown in Fig. 1 were adjusted with the values presented in [26], where R_c and L_c were calculated using real data. The values of the elements of the circuit are given in Appendix.

In this paper, the dynamic model of the electric arc presented in [29] is used. The electric arc is modeled as a controlled voltage source, taking as input the electric arc current. Initially, the radius of the electric arc r is calculated using the non-linear differential equation derived from the energy conservation principle as follows:

$$k_1 r^n + k_2 r \frac{dr}{dt} = \frac{k_3}{r^{m+2}} i^2, \tag{1}$$

where i is the arc current, k_1 is the coefficient of the power transmitted in the form of heat to the external environment, k_2 is the coefficient of the internal power of the electric arc, and k_3 is the coefficient related to the electrical power input. The parameters m and n enable different voltage-current characteristics. The possible combinations of these parameters for the different stages of the arcing process are found in [29]. For the melting stage, these parameters are set as $m = 0$ and $n = 2$. The electric arc voltage v_{arc} is obtained from r using

$$v_{\text{arc}} = \frac{k_3}{r^{m+2}} i. \tag{2}$$

The voltage signal v_{arc} is connected to the electrical power system as a current-controlled voltage source. In practice, the voltage measurements are taken at the secondary side of the transformer T_2, which is

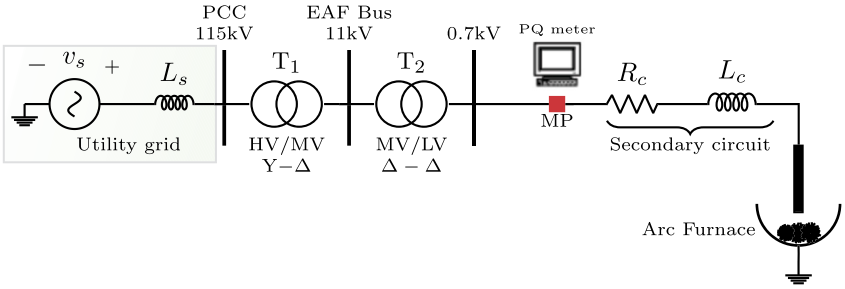

Fig. 1. Single-phase circuit diagram of the EAF power system under study.

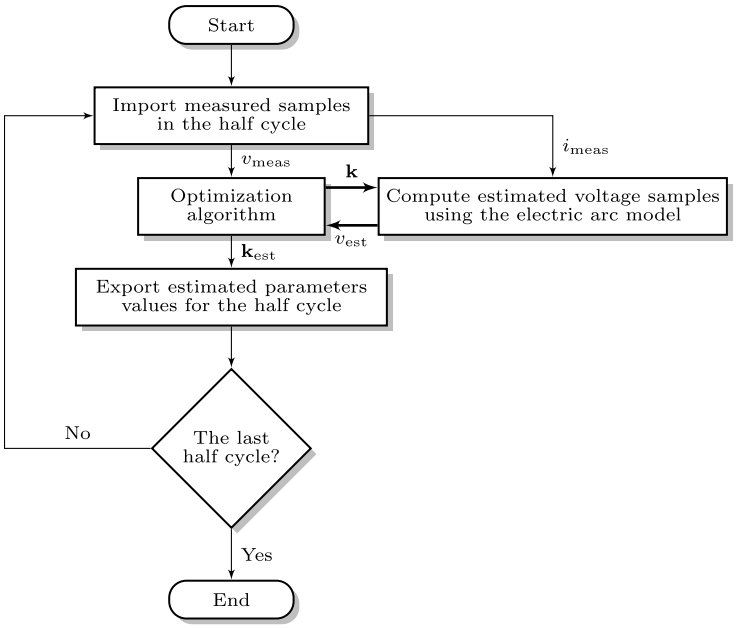

Fig. 2. Flowchart diagram of the proposed method used to estimate the parameters of the electric arc model.

indicated as the measurement point (MP) in Fig. 1. In this paper, the phase voltage at this place is denoted as v, its relationship with v_{arc} and i is given by

$$v = R_c i + L_c \frac{di}{dt} + v_{\text{arc}}, \tag{3}$$

where R_c and L_c are the values of resistance and inductance, respectively, of the secondary circuit including flexible cables, bus tubes and the impedance of the electrodes. These values were calculated in [26], and the results obtained are used in this work.

In brief, based on (1) and (2), the parameters of the electric arc model to be estimated are k_1, k_2 and k_3. Notice that, the parameters m and n are tuned depending on the operating phase of the EAF, and are not considered in the parameter estimation process. To facilitate the description of meta-heuristic algorithms used, it is convenient to define the vector $\mathbf{k} = [k_1, k_2, k_3]^\top$, whose entries are the parameters to be estimated.

3. Model parameters estimation

The main objective of this paper is to estimate the vector of electric arc parameters $\mathbf{k}$ described in the previous section, using real measurements of voltage and current taken at the MP of the EAF electrical circuit as shown in Fig. 1. The used methodology considers the parameters varying in each half cycle of the electric arc current. This idea is in accordance with some studies such as [28], [25] and [7]. The authors indicate, despite having a stochastic behavior for the electric arc in a long observation window, it is possible to assume few variations in each half cycle [28,25,7]. They have also indicated when the system controller of a static VAr compensator (SVC) is designed, the reactive power consumed by the arc furnace is assumed time-varying in each half cycle [30]. Therefore, we also assume that the estimation process is carried out separately for each half-cycle.

Different techniques have been used to estimate the parameters of an electric arc model. Among the most outstanding, in [7] and [28] it is assumed the parameter estimation problem is a multi-objective optimization problem using genetic algorithms (GA). The authors, through the GA, minimize two objective functions, which are related to different parameters of the electric arc model such as the extinction voltage and arc resistance [28]. In contrast with the methods presented in [7] and [28], this paper proposes an estimation methodology based on a single-objective optimization problem. The proposed method is shown in Fig. 2.

Specifically, the estimation procedure can be regarded as a constraint minimization problem, that is, [28]

$$\begin{aligned} &\min_{\mathbf{k}\in\Omega} f(\mathbf{k}) = \text{OF}(v_{\text{est.}}(\mathbf{k}), v_{\text{meas.}}) \\ &\qquad s.a \\ &\underline{\mathbf{k}} \leq \mathbf{k} \leq \bar{\mathbf{k}} \end{aligned} \tag{4}$$

where $\underline{\mathbf{k}}$ and $\bar{\mathbf{k}}$ are the lower and upper limit of $\mathbf{k}$, respectively. The objective function (OF) calculates the mean value of the rooted sum of squared errors between the measured voltage v_{meas_i} and the estimated voltage v_{est_i} samples of the voltage at the secondary side of the EAF transformer, as follows [7], [28]:

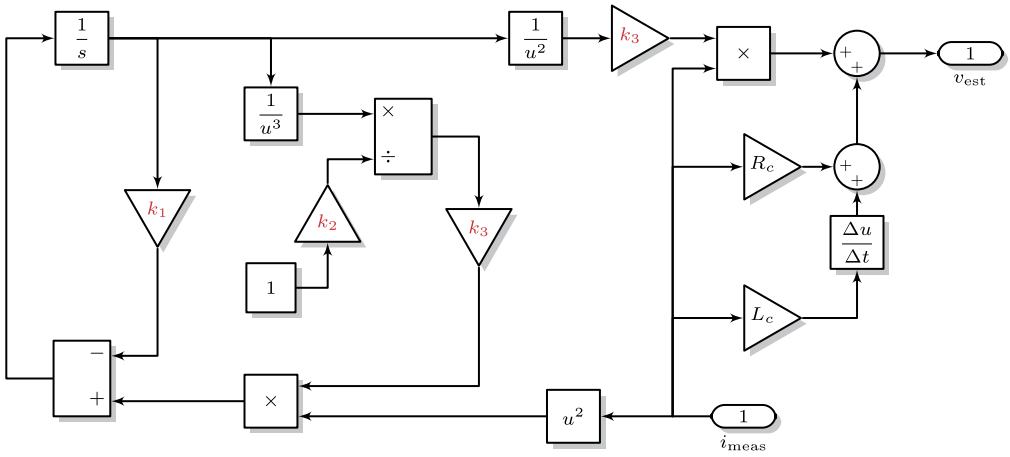

Fig. 3. Implementation in Matlab-Simulink of the dynamic electric arc model, based on energy conservation principle, with $m = 0$ and $n = 2$.

$$\mathrm{OF} = \frac{1}{N}\sqrt{\sum_{i=1}^{N}(v_{\mathrm{est}_i}(\mathbf{k}) - v_{\mathrm{meas}_i})^2} \tag{5}$$

where N is the number of samples in each half cycle. The estimated arc voltage is computed using the measured samples of the electric arc current as input to the electric arc model, named as i_{meas}, then using the equations (1), (2) and (3), the estimated voltage is calculated. This OF was used in [7], [28] to define one of the objective functions to be minimized in the estimation of the parameters of an electric arc model. Fig. 3 shows the Matlab/Simulink implementation of the block diagram to obtain at the output the samples of v_{est}, with $m = 0$ and $n = 2$ (melting phase), and taking as input the samples of i_{meas}.

To solve the problem shown in Eq. (4), several meta-heuristic algorithms have been used. These methods attempt to minimize a fitness function or objective function, by searching the model parameters on search space Ω, which is limited by predefined intervals formed by the possible solutions of the arc furnace parameters. The vast majority of meta-heuristic methods attempt to follow natural, physical or biological principles. Thus, these methods find near-optimal solutions, do not use gradients or Hessians to compute optimal solutions and can apply to a wide class of optimization problems. In the next subsections, we explain briefly how to work meta-heuristic approaches in the context of parameter estimation in an electric arc model.

3.1. Particle swarm optimization

PSO is a population-based search method that follows the biological community nature that exhibits both individual and social behavior such as flocks of birds, schools of fishes and swarms of bees [31]. This technique can be considered the most popular of meta-heuristic techniques and is based on the interaction of a swarm of particles, known as a swarm, with each member of the swarm being associated with a position vector $\mathbf{x}_t$ and a velocity vector $\mathbf{v}_t$ [31]. The size of $\mathbf{x}_t$ and $\mathbf{v}_t$ is equal to the dimension of the search space. Here, $\mathbf{v}_t$, called a history term, represents the directional distance that the particle has covered in the $(t-1)^{\mathrm{th}}$ iteration.

The velocity of each population member, that move into the search space, depends on previous $\mathbf{v}_t$, the particle's personal-best ($\mathbf{k}_l$) and the swarm's best ($\mathbf{k}_g$), that is, it is given as,

$$\mathbf{v}_{i,t+1} = w\mathbf{v}_{i,t} + c_1\mathbf{r}_1 .* (\mathbf{k}_{l,i} - \mathbf{x}_{i,t}) + c_2\mathbf{r}_2 .* (\mathbf{k}_g - \mathbf{x}_{i,t}), \tag{6}$$

$$\mathbf{x}_{i,t+1} = \mathbf{x}_{i,t} + \mathbf{v}_{i,t+1} \tag{7}$$

where $c_1 \in \mathbb{R}$ and $c_2 \in \mathbb{R}$ are constants influencing the best local and global solutions; w is a parameter (it is called the inertia weight constant) that controls the impact of the previous velocity of a particle over the current one, impacting the exploration capacities of the algorithm. Finally, $\mathbf{r}_1$ and $\mathbf{r}_2$ are two parameters that introduce randomness, from the uniform distribution ($\mathbf{r}_1, \mathbf{r}_2 \sim \mathcal{U}[0,1]$), into the search process.

The method could be summarized as follows: the swarm is initialized, considering the restrictions of the problem; then the quality, using the objective function, of each particle is evaluated and $\mathbf{k}_g$, and $\mathbf{k}_i$ are initialized; for each iteration the velocity and position of each particle are updated using Eq. (6) and (7), then the quality of each particle is evaluated, next $\mathbf{k}_g$ and $\mathbf{k}_i$ are updated if needed; and w is decreased. This process is repeated until either a stopping criterion is reached or a minimum fitness value is obtained by a particle in the swarm. In the above description, the vector $\mathbf{k}_i$ is composed by the parameters k_1, k_2 and k_3.

3.2. Vortex search algorithm

The VSA is a meta-heuristic approach that follows the vortex pattern inspiration created by the vortical flow of the stirred fluids. The VSA applies the generation and replacement procedures to propose a new candidate solution of the optimization problem. In the generation procedure, a set of candidate solutions is generated from the previous solution by using a multivariate Gaussian distribution. During the replacement phase, a solution is chosen from the candidate solutions to supply the previous solution set [32].

3.2.1. Proposing new candidate solutions

For generating new candidate solutions, the VSA computes an initial center $\hat{\mathbf{k}}_0$ to generate randomly a number of solutions from the previous solution. $\hat{\mathbf{k}}_0$ is the midpoint of the search space. Using this center, a multivariate Gaussian distribution is employed to generate new candidate solutions, where the covariance matrix is based on the upper limit and lower limit of the decision variables [32], that is, the VSA assumes that a new solution is generated by

$$\mathbf{k} \sim \mathcal{N}\left(\mathbf{k}\middle|\hat{\mathbf{k}}, \boldsymbol{\Sigma}\right), \tag{8}$$

where $\mathbf{k} \in \mathbb{R}^{d\times 1}$ is a candidate solution; $\hat{\mathbf{k}} \in \mathbb{R}^{d\times 1}$ is the vortex center; and $\boldsymbol{\Sigma} \in \mathbb{R}^{d\times d}$ is the covariance matrix. According to [32], the search space is modified using $\boldsymbol{\Sigma}$. Here, we use a diagonal covariance matrix with σ^2 that controls the radio of contours of probability density for the Gaussian distribution. The idea behind the VSA is to improve the center and radio of the search space contour in each iteration.

3.2.2. Replacement of the current solution

Once we have generated new candidate solutions, these solutions must be ensured to be inside the search boundaries. Next, it is necessary to replace the current center $\hat{\mathbf{k}}_{t-1}$ of the search space contour and then,

a new set of candidate solutions is generated around the new center $\hat{\mathbf{k}}_t$. To replace $\hat{\mathbf{k}}_{t-1}$ the memorized best solution is assigned to be the new center $\hat{\mathbf{k}}_t$. This process is repeated until the stopping criterion is satisfied [32]. Once the algorithm has finished, the center of the smallest circle is the optimum point found by the algorithm. Therefore, the VSA only memorizes the best solution and the radius of the center is iteratively decreased. This process of the memorization is similar to several search-based meta-heuristic approaches, for example the Pattern Search and the iterated local search algorithm. For more information, see [32]. In our case, the vector $\hat{\mathbf{k}}_t$ is composed by the parameters k_1, k_2 and k_3.

3.3. Crow search algorithm

The CSA is a meta-heuristic optimizer that follows the behavior of crows, which are considered as the most intelligent birds [33]. The idea behind this algorithm is the crows store their excess food in safe places and retrieve it when the food is needed. Additionally, they live in the form of flock, remind the position of their safe places, follow each other to obtain food and they conserve these safe places. For applying the CSA, it is necessary to define a flock of crows where each crow denotes a feasible solution of the problem. For each crow, the new position of crow $\mathbf{k}_i^{g+1}$ is obtained as follows,

$$\mathbf{k}_i^{g+1} = \mathbf{k}_i^g + r_i fl_i^g \left(\mathbf{m}_i^g - \mathbf{k}_i^g\right), \tag{9}$$

where r is a constant that introduces uncertainty, which is considered as a uniform random variable between 0 and 1; fl_i^g is the flight length of crow i at iteration g; and $\mathbf{m}_i^g$ is considered a safe place (or a better food place) at iteration g. In the CSA, the balance between exploration and exploitation is controlled by a parameter of awareness probability α_{AP} [33] over the Eq. (9), that is, if $r_i \geq \alpha_{AP}$, the CSA updates the position $\mathbf{k}_i^g$ using the Eq. (9) or explores the search space on a global scale. Otherwise, the CSA examines the local region where a current good solution is found. To estimate the parameters k_1, k_2 and k_3, we use the best position of crow $\mathbf{k}_i$.

3.4. Genetic algorithm

The GA was first applied by Holland in 1975 [34]. It was inspired in the Darwin's theory of evolution, imitating the biological evolution of the living organism. The algorithm starts with a population of candidate solutions also called chromosomes, which are represented as a vector $\mathbf{k}$, the entries of which are the genes k_j, $j \in \{1,2,3\}$, that are created from random values of the parameters to be estimated, within the domain $[k_j^{\min}, k_j^{\max}]$ previously defined. The number of chromosomes in each generation is referred to as the population size [28,35]. The population evolves in each generation, by using selection, crossover and mutation operations. The selection strategy is applied to choose the parents for the next generation, as described below.

First, the fitness of each chromosome of the current population is calculated using the fitness function given by (5). After the evaluation of all the population, those chromosomes which have better fitness values are selected as parents to create the next population. The stochastic universal sampling strategy is utilized as selection function, this method is comparable to using a roulette wheel in a casino, where each chromosome in the population has a slot of the wheel proportional to its fitness value. The roulette wheel is divided into a number of equally spaced selection points around it. A single spin of the weighted roulette wheel yields the parents candidate, by selecting the slots below the selection points. In this way, more highly fit chromosomes have more opportunities to survive into the succeeding generation [36]. It is should be noted that, a percentage of the chromosomes at the current population with the best fitness values are chosen as the elite, and its genes survive to the next generation. The value of these percentages is referred as the "elite individuals". A crossover operation is utilized to extract the best genes from different individuals and recombine them to increase the quality of chromosomes for the next generation. The number of individuals that are created using the crossover rule is computed by the value of the parameter "crossover fraction". The crossover operator used in this study, combines two chromosomes at the current generation, to form a new crossover chromosome of the offspring. For this procedure, a crossover point within the genes is chosen at random. The mutation operator is used to create the mutation chromosomes of the offspring, that allow to maintain diversity in the population, and enables the GA to search in a broader space [35]. In this study, it is used the mutation operation described in [37], in which a fraction of the chromosomes of the current population is taken to make a small random changes over its genes, by adding a random number taken from a Gaussian distribution which has a mean of 0 and a standard deviation computed according to

$$\sigma_{j,g} = \sigma_{j,g-1}\left(1 - \frac{g}{g^{\max}}\right) \tag{10}$$

where $\sigma_{j,g}$ is the standard deviation at the g^{th} generation and at coordinate j of the parent vector $\mathbf{k}$, and $g^{\max}$ is the maximum number of generations. The standard deviation at the first generation is given by $\sigma_{j,0} = k_j^{\max} - k_j^{\min}$.

The algorithm is repeated until emerges a candidate solution that satisfies a predefined criterion. In this paper, the algorithm is stopped when the maximum number of generation defined by the user is reached.

3.5. Differential evolution algorithm

The DE algorithm was proposed in 1997 by Storn and Price [38] as a meta-heuristic optimization algorithm, which maintains a population of potential solutions in the search space by applying the idea of survival of the fittest. In this case, the search space is formed by predefined intervals for values of the electric arc model parameters. The main advantages of DE is its convenient implementation, lack of a differentiable cost function, good converge properties, and few control variables to achieve the minimization.

The DE algorithm makes use of three main rules: mutation, crossover, and selection. Initially, a population is generated. Each individual of the population has following structure:

$$\mathbf{k}^g = [k_1^g, k_2^g, k_3^g] \tag{11}$$

where g represents the g^{th} generation.

In the mutation rule a mutant vector is created following the rule:

$$\hat{\mathbf{k}}^{g+1} = \mathbf{k}_1^g + m_t(\mathbf{k}_2^g - \mathbf{k}_3^g) \tag{12}$$

where m_t is a mutation factor $\in [0, 1.2]$, and $\mathbf{k}_1^g$, $\mathbf{k}_2^g$, $\mathbf{k}_3^g$, are three random vectors taken from the population in the g^{th} generation.

The crossover rule generates a trial vector $\mathbf{k}^{g+1}$, where each one of its entries is computed as follows:

$$k_j^{g+1} = \begin{cases} \hat{k}_j^{g+1}, & \text{if } \vartheta \leq cr \\ k_j^g, & \text{otherwise} \end{cases} \tag{13}$$

for $j = 1,2,3$. ϑ is a random variable which follows a normal distribution in the range $[0,1]$, and cr is known as crossover constant.

The selection rule compares the value of the OF given by (5) for the trial vector and the OF for the target vector $\mathbf{k}^g$, and select the best solution that is stored in the population for the next generation $(g+1)$, as follows

$$\mathbf{k}^{g+1} = \begin{cases} \mathbf{k}^{g+1}, & \text{if } \text{OF}(\mathbf{k}^{g+1}) \leq \text{OF}(\mathbf{k}^g) \\ \mathbf{k}^g, & \text{otherwise} \end{cases} \tag{14}$$

The above procedure is repeated for each individual of the population. The algorithm stops when the number of maximum generations $g^{\max}$ defined by the user is reached.

3.6. Least squares method

There is other methodology proposed in the literature [25], different to the meta-heuristics algorithms, that has been used to estimate the parameters of the electric arc model in each half cycle, based on a transformation of the non-linear differential equation that describes the dynamic behavior of the v-i characteristic of the model, into a linear equation whose solution can be done by LSM. In effect, replacing (2) in (1), and with $m = 0$ and $n = 2$, following equation is obtained

$$k_1 r^2 + k_2 r \frac{dr}{dt} = v_{\text{arc}} i \tag{15}$$

From (2), the arc radius can be expressed in terms of a new variable u as:

$$r = k_3^{\frac{1}{2}} u \tag{16}$$

where the variable u depend of the real measurements of arc voltage and arc current as follows

$$u = \left(\frac{i}{v_{\text{arc}}} \right)^{\frac{1}{2}} \tag{17}$$

replacing (16) in (15), result the following equation

$$k_1 k_3 u^2 + k_2 k_3 u \frac{du}{dt} = v_{\text{arc}} i \tag{18}$$

the above equation can be written in the form of a linear regression model, as follows

$$a x_1 + b x_2 = y \tag{19}$$

where

$$\begin{cases} x_1 = k_1 k_3 \\ x_2 = k_2 k_3 \\ a = u^2 \\ b = u \frac{du}{dt} \\ y = v_{\text{arc}} i \end{cases} \tag{20}$$

Notice that, it is possible compute the values of a and b for each sample of real measurement of the electric arc current i, and the phase voltage v. Considering N samples of real measurements of arc voltage and arc current in each half cycle, (19) is rewritten as,

$$\begin{bmatrix} a_1 & b_1 \\ a_2 & b_2 \\ \vdots & \vdots \\ a_N & b_N \end{bmatrix} \begin{bmatrix} x_1 \\ x_2 \end{bmatrix} = \begin{bmatrix} y_1 \\ y_2 \\ \vdots \\ y_N \end{bmatrix} \tag{21}$$

The above equation is of the form $\mathbf{Ax} = \mathbf{y}$. The solution vector $\mathbf{x}^*$ that minimize the residual error, can be calculated with linear least square method, from $\mathbf{x}^* = (\mathbf{A}^\top \mathbf{A})^{-1} \mathbf{y}$. In this method, it is necessary to adjust previously the value of k_3 to compute the values of k_1 and k_2, using $k_1 = x_1/k_3$ and $k_2 = x_2/k_3$, where x_1 and x_2 are the entries of the vector $\mathbf{x}^*$.

4. Results and discussion

This section presents the results obtained from the proposed methodologies to estimate the parameters of the arc furnace model, which are based on the meta-heuristic optimization algorithms. The description of the real data of phase voltage and arc current, that it is used in the estimation process, is presented in the subsection 4.1. In subsection 4.2, the hyperparameters and the performance comparison of the different meta-heuristic algorithms are also displayed. Finally, in subsection 4.3, the best estimated parameters obtained for the electric arc model, and the comparison between the real and simulated voltage and current waveform are shown.

Table 1
Lower and upper bound of each one of the parameters to be estimate.

Parameter	Lower Limit	Upper Limit
k_1	1000	5000
k_2	1	5
k_3	10	30

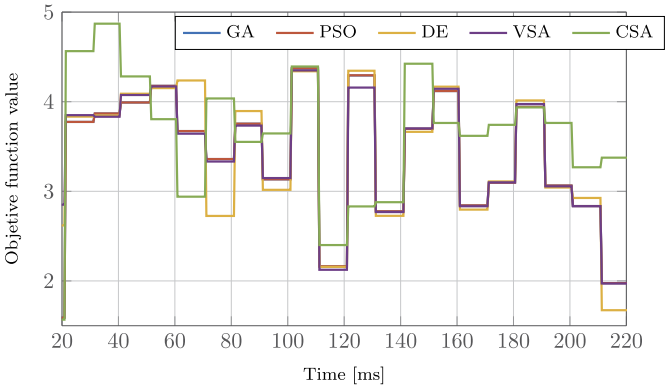

Fig. 4. Values of the objective function in each cycle of GA, ED, PSO, VSA and CSA, for optimizing the fitness function.

4.1. Real data used to estimate the parameters of the model

In order to test all the proposed methodologies, real data were taken from the secondary side of the transformer T_2 in the power system as shown in Fig. 1. These data correspond to the phase voltage and the arc current. A PQ meter (AEMC 8333 Power Pad III) connected at phase A of the MP, was used to measure ten consecutive cycles (or 20 half cycles) of voltage and current at fundamental frequency of 50 Hz. The measurements have a fixed sampling rate of 8192 samples per second, it were taken during several seconds in the melting phase of the arc furnace operation, and ten consecutive cycles were randomly selected to evaluate the predictive performance of the methods considered.

4.2. Performance comparison of the algorithms

After having analyzed how the data were captured, all the meta-heuristic algorithms were applied them as explained in section 3. Here, all the algorithms were executed with a population size of 30, and a maximum number of generations (or iterations) of 100, which correspond to typical values as shown in [28]. The remaining algorithm parameters were adjusted as follows. In the PSO algorithm, c_1 and c_2 were both fixed in 2, and $\omega = 1.1$. In CSA, f_l and α_{AP} were adjusted as $f_l = 1.2$ and $\alpha_{AP} = 0.1$. In GA, the crossover fraction was set to 0.8, elite individuals were of 5% of the population, and the tolerance was set to 0.01. In the DE algorithm were set $m_t = 0.8$ and $cr = 0.5$.

As mentioned in Section 3, the search space of optimization algorithms Ω is limited by the intervals $[k_j^{\max}, k_j^{\min}]$ where $j \in \{1, 2, 3\}$. In Table 1, the lower and upper limits for each one of the model parameters are shown. These values correspond to typical values reported in previous studies as in [26] and [39]. With the data in Table 1, the proposed algorithms were applied to the real data described above. Fig. 4 shows the behavior of the methods in terms of the objective function.

From Fig. 4 note that the optimal OF values are similar in each half cycle, there is no single meta-heuristic algorithm that will always provide the minimum OF value in all the half cycles. Also noted that, the GA, VSA and PSO present comparable behavior in all the observation windows.

To notice the differences among the methods, in Table 2 are reported the average value of the OF values shown in Fig. 4. This average

Table 2
Average value of the OF function, error indices of voltage and current, and running time for the studied methods.

Method	OF_{avg}	$RMSE_{avg}$	E_v	E_i	UEI	Running time [min]
PSO	**3.42** ± 0.68	**30.96** ± 6.16	**0.25**	**0.08**	**0.16**	**2.37** ± 0.72
VSA	3.43 ± 0.67	31 ± 6.04	0.25	0.08	0.17	3.32 ± 0.12
CSA	3.68 ± 0.64	33.33 ± 5.82	0.36	0.10	0.23	3.32 ± 0.15
GA	**3.42** ± 0.68	**30.96** ± 6.16	**0.25**	**0.08**	**0.16**	3.32 ± 0.74
DE	3.42 ± 0.76	30.97 ± 6.86	0.26	0.08	0.17	12.7 ± 0.80
LSM	–	–	7.68	0.16	3.92	20μ ± 4.0μ

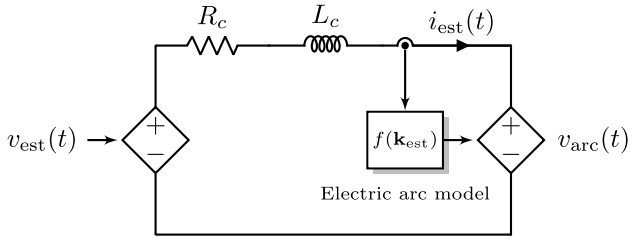

Fig. 5. Single-phase diagram of the secondary circuit at transformer T_2, implemented in Matlab/Simulink.

value is named as OF_{avg}. Notice that, the OF_{avg} obtained by all the algorithms are very similar (around 3.5), being the running time for each half cycle the unique difference between them. The running time in the estimation process for each half cycle has been computed using a desktop computer with an Intel(R) Core(TM) processor i7-3612QM CPU @ 2.10 GHz. From Table 2, the PSO obtained the lowest running time. The root mean square error (RMSE) given by (22) was used to evaluate the estimation performance of the algorithms considered. Similar to the OF, the RMSE changes in every half cycle, therefore its average value is reported in Table 2. The relationship between the OF (5) and RMSE (22) is given by $\text{RMSE} = \sqrt{N}\text{OF}$, the unique difference between them is the scale factor $\sqrt{N}$, therefore the results obtained for each algorithm maintain the same trend.

$$\text{RMSE} = \sqrt{\frac{\sum_{i=1}^{N}(v_{\text{est}_i}(\mathbf{k}) - v_{\text{meas}_i})^2}{N}} \tag{22}$$

The error index shown in (23), which is defined by [25], has been used to evaluated the performance of the meta-heuristic algorithms.

$$E_x = \frac{1}{L \times d}\sum_{1}^{L}\sum_{1}^{d}\frac{x_{\text{meas},k} - x_{\text{est},k}}{|x_{\text{meas},k}|} \tag{23}$$

where x represents a voltage or current signal, d is the number of samples in each half cycle, L is the number of half cycles of real measurement signals, $x_{\text{meas},k}$ represent the k^{th} sample of real signal, and $x_{\text{est},k}$ is the k^{th} sample of estimated signal. To compute the estimated electric arc current i_{est}, it is used the electrical circuit shown in Fig. 5, which has two controlled voltage sources. The voltage of the left source corresponds to the estimated voltage v_{est} (i.e. phase voltage at the secondary side of transformer T_2), which is computed using the measured current i_{meas} and the estimated parameters, as shown in Fig. 3. The voltage of the right source corresponds to the electric arc voltage v_{arc}, which is calculated using Eqs. (1) and (2), taking as input the estimated arc current $i_{\text{est}}(t)$ and the estimated parameters $\mathbf{k}_{\text{est}}$.

On the other hand, a unified error index (UEI) was used to group in a single error the error index of voltage (E_v) and the error index of the current (E_i) as is shown in [25]. The UEI is defined as follows

$$\text{UEI} = \frac{|E_v| + |E_i|}{2} \tag{24}$$

Returning to Table 2, it can be observed that the GA and PSO present the minimum values for the E_v, E_i and the UEI. From the values of UEI calculated by all the methods considered, it is very clear that LSM obtained the worst performance. However, the LSM requires around 20 μs to perform the parameters estimation. It is worth mentioned that the values of the UEI index obtained with the meta-heuristic algorithms are lower than the UEI values reported in [25].

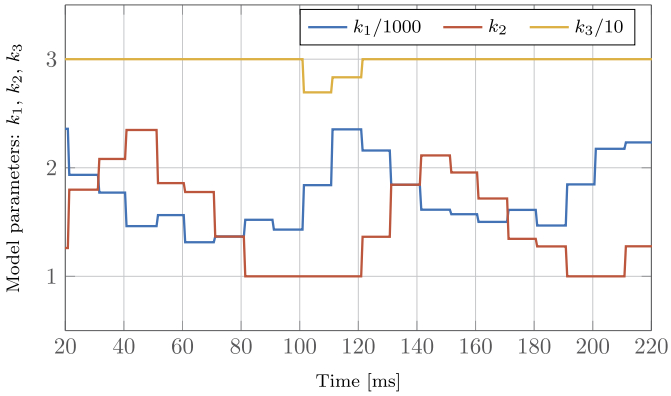

Fig. 6. Optimal values for the parameters k_1, k_2 and k_3, obtained by the PSO algorithm.

In brief, the performance of the meta-heuristic algorithms utilized is very similar, but it is necessary to take into account the running time, where the PSO obtained the best performance. Due to the performance shown by the PSO, the rest of the results are reported with the estimated parameters obtained with this technique.

4.3. Real and simulated voltage and current waveform with the best estimated parameters

After having shown the application of the different methods to estimate the parameters of the system, we are going to present the optimal parameters k_1, k_2 and k_3 in each half cycle during the observation window, obtained with the PSO algorithm. In Fig. 6, it is possible to note that the parameter k_3 is equal to 3 during the major part of the observation window. The parameters k_1 and k_2 change with an aperiodic behavior, as expected in this type of loads. That is, the electric arc dynamic is focused on the variation of the parameters k_1 and k_2. This time-varying behavior is analyzed in [25] using an auto regressive moving average model.

Fig. 7 shows ten cycles of the measurement and estimated samples of phase voltage taken at the MP, when the parameters k_1, k_2 and k_3 are adjusting in each half cycle with the values shown in Fig. 6. As can be seen, the estimated samples of the phase voltage are very similar with the real samples in all the observation window. The difference between each sample of the real and simulated voltage is shown in Fig. 7. The RMSE between these signals is 0.0188 kV, which is according to the small difference during the major part of the observation window between these signals. The maximum absolute value of the difference is 0.09 kV and occurs in $t = 60.9$ ms, when the value of the actual voltage is 0.4 kV.

Fig. 8 displays ten cycles of the measurement and estimated samples of the electric arc current taken at the MP. As can be seen, the estimated samples of the current can capture the non-sinusoidal and time-varying random behavior that exhibit the real samples. Also, the figure shows the difference between each sample of measurement and estimated samples. The RMSE between these signals is 5.33 kA. Notice that, the maximum difference is 10.9 kA, and occurs in $t = 133.6$ ms, when the actual sample of the arc current is equal to −73.74 kA, as can be seen in the figure at the right.

Fig. 9 (a) shows the measurement and estimate voltage-current characteristic, using the samples of the phase voltage and the arc current at the secondary side of T_2 transformer (see Fig. 1). Fig. 9 (b) shows the voltage-current characteristic of the electric arc, where the arc voltage has been calculated by solving the Eq. (3) for v_{arc}, due to it is not

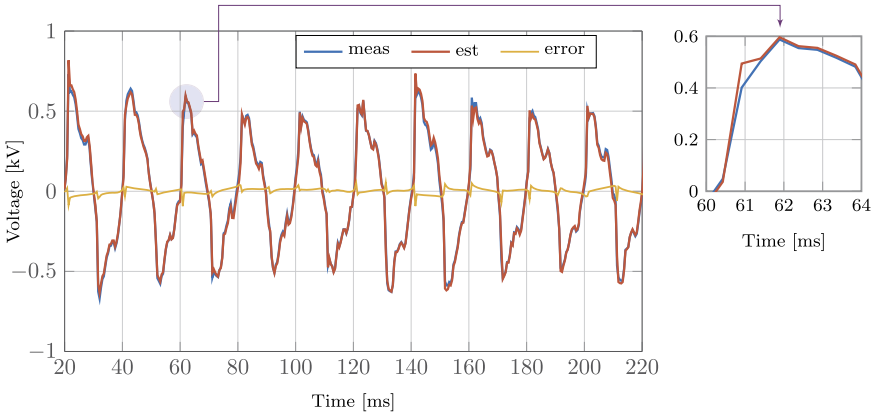

Fig. 7. Measurement (meas) and estimated (est) phase voltage, adjusting the model parameters with the PSO algorithm.

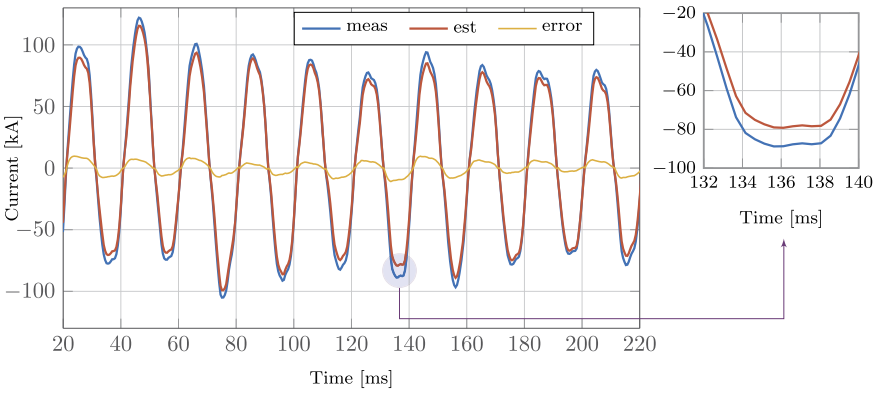

Fig. 8. Measurement (meas) and estimated (est) arc current, adjusting the model parameters with the PSO algorithm.

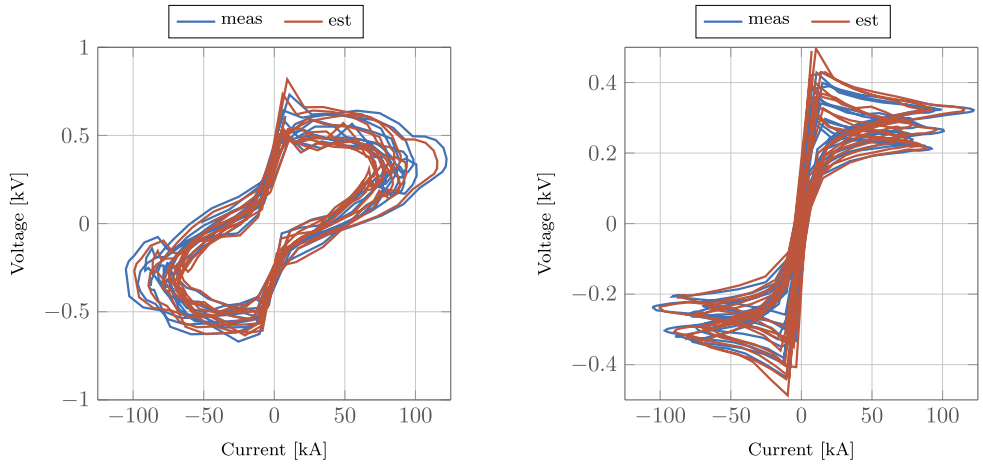

(a) V-I characteristic in the MP. (a) V-I characteristic of the electric arc.

Fig. 9. Measurement (meas) and estimated (est) voltage-current characteristic, during the melting stage of the arc furnace operation, (a) at MP, (b) at the electric arc.

possible to obtain measurements of the electric arc voltage directly. The "measurement" (meas) arc voltage has been calculated using the voltage and current at the MP, and the estimated (est) arc voltage has been calculated using the estimated voltage and current samples at the MP. Notice that the electric arc model used is able to capture the non-linearity between the voltage and the arc current. These results validate the proposed methodology for estimating the parameters k_1, k_2 and k_3.

Once the estimates of the voltage and current signals had been validated, an analysis of the harmonics present in these two signals was performed. Therefore, the short-time Fourier transform (STFT) has been used to compute the harmonics of the real and estimated waveforms of voltage and current. The STFT has been computed considering the harmonics and interharmonics of the measurement and estimate signal. Each segment of the signal is windowed with a Hamming window of 5-Hz resolution, with an overlap of 90% between the segments. The considered frequencies have a range of 5 to 650 Hz, with steps of 5 Hz for 5 Hz to 100 Hz, and 50 Hz for larger frequencies. The STFT of a signal x is a matrix $\mathbf{S}_x$, where each column of $\mathbf{S}_x$ contains the short-time, time-localized frequency content of x. The magnitude of each element of the resulting matrix has been averaged over its columns.

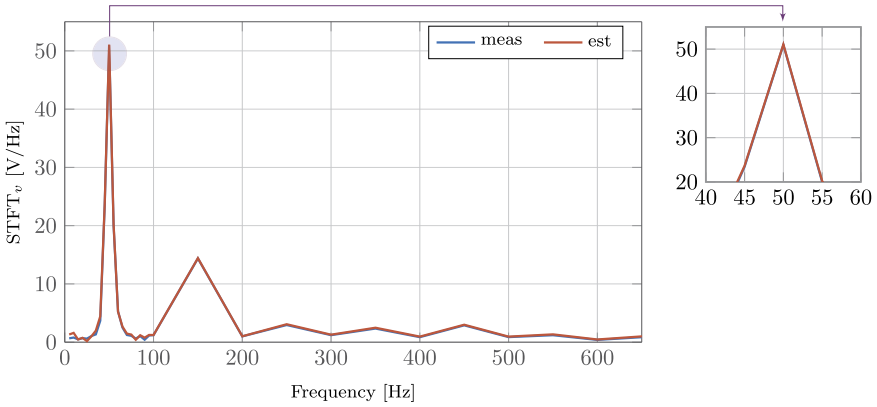

Fig. 10. Measurement (meas) and estimated (est) spectrogram of the phase voltage, during the melting stage of the arc furnace operation.

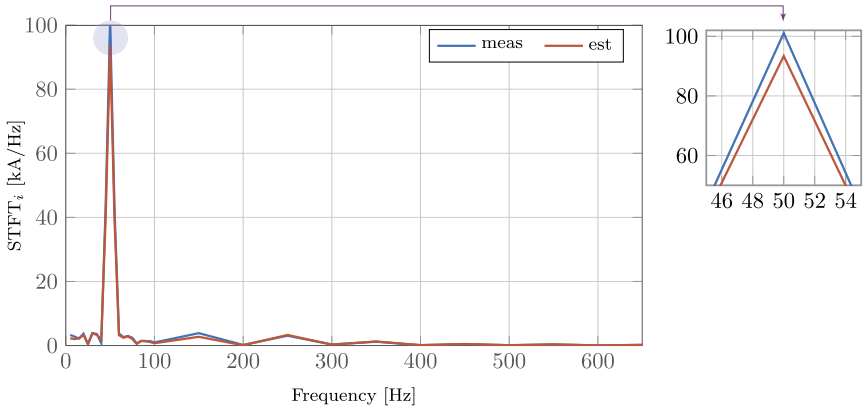

Fig. 11. Measurement (meas) and estimated (est) spectrogram of arc current, during the melting stage of the arc furnace operation.

The result is a vector $\mathbf{s}_x \in \mathbb{R}^{31\times1}$, where 31 correspond to the number of frequencies considered. In this paper, the command spectrogram of Matlab has been used for computing the STFT of the signals. In Fig. 10, the averaged spectrogram of the measurement and estimated voltage are shown. As can be seen, the spectrum of both signals are very similar through of the range of frequencies considered, the fundamental component at 50 Hz, has been zoomed in Fig. 10 to show the similitude in this component. The relative error between the measurement and estimated fundamental component is 0.22%. In the same way, the spectrogram of the measurement and estimated arc current are shown in Fig. 11. The fundamental component has been zoomed in the same figure. The relative error between the measurement and estimated fundamental component of the arc current is 7.6%. The authors consider that this result is a good approximation due to randomness present in the measured current.

The total harmonic distortion (THD) index has been considered to evaluate the distortion of the measured and estimated signals of the voltage and current. THD is calculated according to the definition given in the IEEE standard 519-2014, where the first 20 harmonics have been taken into account in the calculation. The equation used to calculate the THD is shown in Eq. (25)

$$\mathrm{THD}_s = \left(\frac{1}{s_1} \sqrt{\sum_{\substack{k=2,\\ k\neq1}}^{20} s_k^2} \right) \cdot 100\% \tag{25}$$

where s_k is the k^{th} component of the vector $\mathbf{s}$, and s_1 is the main component at the frequency of 50 Hz. Those components have been calculated using the discrete Fourier transform. Table 3 presents a comparison between the mean value and the standard deviation of the THD values calculated in each cycle of the measured and estimated voltage and current signals shown in Fig. 7 and Fig. 8. The relative errors between the THD of measured and estimated signals of voltages and arc currents are 0.3% and 1.91%, respectively, which demonstrate the coincidences between the measured and estimated signals. These relative errors are smaller than the corresponding errors reported in [26].

Table 3
Comparison between the THD index of the spectrum of the measured and estimated voltage and current.

	measured	estimated	relative error of the mean value
THD_v	$33.05\% \pm 3.66\%$	$33.15\% \pm 3.77\%$	0.3%
THD_i	$7.83\% \pm 1.7\%$	$7.98\% \pm 1.6\%$	1.91%

5. Conclusions

This paper presents the performance comparison of the five most commonly used meta-heuristic optimization algorithms, used to estimate the parameters of an EAF model. A half cycle estimation approach of the measured signal was used, which is consistent with the ideas presented in previously published studies as [5,28,25,7]. Three algorithms were considered as new alternatives to optimize the parameter estimation of an electric arc furnace model: PSO, VSA and CSA algorithms. Their results were compared with two state-of-art approaches: GA [28,7], and LSM [25]. After adjusting the parameters of the electric arc model with the estimated parameters, the model was run to obtain the simulated signals of voltage and current. Error indices and running time were considered in order to compare the performance of the studied algorithms. According to the results, the PSO algorithm presented the best performance to estimate the parameters of an electric arc furnace model, the PSO algorithm is capable to estimate the parameters

with the lowest running time and error rates. Likewise, the simulated signals shown that their nonlinear and time-varying characteristics can be captured by the simulated signals generated by the model. Finally, the proposed methodology allowed to estimate the parameters of the electric arc furnace model by optimizing a single optimization function, in contrast to the proposed methods presented in [28] and [7], in which the estimation process is performed by minimizing two objectives functions, which leads to an increase in computational time. With the proposed methodology of this paper, the computation time in the estimation process is reduced, with low error indexes. As future work, the authors recommend the use of the proposed method to calibrate the parameters of any parametric system described by nonlinear equations. Also, it is necessary to emphasize the following: hyper-parameters of the meta-heuristic algorithms such as c_1, c_2, ω, f_l or α_{AP} must be carefully selected to obtain a satisfactory estimate. Therefore, it is recommended to investigate parameter-free optimization methodologies [40,41] to estimate the parameters of the system.

CRediT authorship contribution statement

J.J. Marulanda-Durango: Data curation, Formal analysis, Investigation, Methodology, Resources, Visualization, Writing – original draft, Writing – review & editing. **C.D. Zuluaga-Ríos:** Conceptualization, Formal analysis, Investigation, Project administration, Resources, Supervision, Validation, Writing – original draft, Writing – review & editing.

Declaration of competing interest

The authors declare that they have no known competing financial interests or personal relationships that could have appeared to influence the work reported in this paper.

Data availability

Data will be made available on request.

Acknowledgement

This work was funded by the Vicerrectoría de Investigación, Innovación y Extensión of the Universidad Tecnológica de Pereira through the proyect: “Implementación de un sistema de control sensorless para un SVC usando modelos dinámicos de carga” (grant 6-22-3).

Appendix A. Parameters of electric arc furnace installation shown in Fig. 1

Utility grid: Ideal three-phase sinusoidal ac voltage with phase to phase RMS nominal voltage 115 kV, X/R ratio: 10. **Transformer T_1:** $\epsilon_{cc} = 12\%$, nominal power: 42 MVA, X/R ratio: 10. **Transformer T_2:** $\epsilon_{cc} = 10\%$, nominal power: 30 MVA, X/R ratio: 10. **Secondary circuit:** $R_c = 0.2$ mΩ, $L_c = 8$ μH.

References

[1] R. Horton, T.A. Haskew, R.F. Burch IV, A time-domain ac electric arc furnace model for flicker planning studies, IEEE Trans. Power Deliv. 24 (3) (2009) 1450–1457, https://doi.org/10.1109/TPWRD.2008.2007021.

[2] Y.-J. Liu, G.W. Chang, R.-C. Hong, Curve-fitting-based method for modeling voltage-current characteristic of an ac electric arc furnace, Electr. Power Syst. Res. 80 (5) (2010) 572–581, https://doi.org/10.1016/j.epsr.2009.10.015.

[3] L. Hocine, D. Yacine, B. Kamel, K.M. Samira, Improvement of electrical arc furnace operation with an appropriate model, Energy 34 (9) (2009) 1207–1214, https://doi.org/10.1016/j.energy.2009.03.003.

[4] M. Cernan, Z. Muller, J. Tlusty, V. Valouch, An improved SVC control for electric arc furnace voltage flicker mitigation, Int. J. Electr. Power Energy Syst. 129 (2021) 106831, https://doi.org/10.1016/j.ijepes.2021.106831.

[5] M. Göl, O. Salor, B. Alboyaci, B. Mutluer, I. Cadirci, M. Ermis, A new field-data-based EAF model for power quality studies, IEEE Trans. Ind. Appl. 46 (3) (2010) 1230–1242, https://doi.org/10.1109/TIA.2010.2046280.

[6] A.T. Teklić, B. Filipović-Grčić, I. Pavić, Modelling of three-phase electric arc furnace for estimation of voltage flicker in power transmission network, Electr. Power Syst. Res. 146 (2017) 218–227.

[7] F. Illahi, I. El-Amin, M.U. Mukhtiar, The application of multiobjective optimization technique to the estimation of electric arc furnace parameters, IEEE Trans. Power Deliv. 33 (4) (2018) 1727–1734.

[8] D.C. Bhonsle, R.B. Kelkar, Analyzing power quality issues in electric arc furnace by modeling, Energy 115 (Part 1) (2016) 830–839.

[9] M.T. Esfahani, B. Vahidi, A new dynamic intelligent time domain arc furnace modeling based on combination adaptive neuro-fuzzy inference system and chain code, Electr. Power Compon. Syst. 44 (11) (2016) 1261–1275, https://doi.org/10.1080/15325008.2016.1158215.

[10] M. Klimas, D. Grabowski, Application of shallow neural networks in electric arc furnace modeling, IEEE Trans. Ind. Appl. 58 (5) (2022) 6814–6823, https://doi.org/10.1109/TIA.2022.3180004.

[11] Y. Wang, Z. Mao, Y. Li, H. Tian, L. Feng, Modeling and parameter identification of an electric arc for the arc furnace, in: 2008 IEEE International Conference on Automation and Logistics, 2008, pp. 740–743.

[12] M. Klimas, D. Grabowski, Application of the deterministic chaos in ac electric arc furnace modeling, in: 2022 IEEE International Conference on Environment and Electrical Engineering and 2022 IEEE Industrial and Commercial Power Systems Europe (EEEIC/I&CPS Europe), 2022, pp. 1–6.

[13] O. Ozgun, A. Abur, Flicker study using a novel arc furnace model, IEEE Trans. Power Deliv. 17 (4) (2002) 1158–1163.

[14] G. Carpinelli, F. Iacovone, A. Russo, P. Varilone, Chaos-based modeling of dc arc furnaces for power quality issues, IEEE Trans. Power Deliv. 19 (4) (2004) 1869–1876.

[15] A.A. Gomez, J.J.M. Durango, A.E. Mejia, Electric arc furnace modeling for power quality analysis, in: 2010 IEEE ANDESCON, 2010, pp. 1–6.

[16] D.A.d.L. Brandao, T.M. Parreiras, I.A. Pires, B.d.J. Cardoso F., Electric arc furnace reactive compensation system using zero harmonic distortion converter, IEEE Trans. Ind. Appl. 58 (5) (2022) 6833–6841, https://doi.org/10.1109/TIA.2022.3187392.

[17] M.T. Esfahani, B. Vahidi, A new stochastic model of electric arc furnace based on hidden Markov model: a study of its effects on the power system, IEEE Trans. Power Deliv. 27 (4) (2012) 1893–1901.

[18] G.W. Chang, C. Chen, Y. Liu, A neural-network-based method of modeling electric arc furnace load for power engineering study, IEEE Trans. Power Syst. 25 (1) (2010) 138–146, https://doi.org/10.1109/TPWRS.2009.2036711.

[19] G.W. Chang, M. Shih, Y. Chen, Y. Liang, A hybrid wavelet transform and neural-network-based approach for modelling dynamic voltage-current characteristics of electric arc furnace, IEEE Trans. Power Deliv. 29 (2) (2014) 815–824, https://doi.org/10.1109/TPWRD.2013.2280397.

[20] C. Chen, Y. Chen, A neural-network-based data-driven nonlinear model on time- and frequency-domain voltage-current characterization for power-quality study, IEEE Trans. Power Deliv. 30 (3) (2015) 1577–1584, https://doi.org/10.1109/TPWRD.2015.2394359.

[21] G.W. Chang, S. Lin, Y. Chen, H. Lu, H. Chen, Y. Chang, An advanced EAF model for voltage fluctuation propagation study, IEEE Trans. Power Deliv. 32 (2) (2017) 980–988.

[22] F. Janabi-Sharifi, G. Jorjani, An adaptive system for modelling and simulation of electrical arc furnaces, Control Eng. Pract. 17 (10) (2009) 1202–1219, https://doi.org/10.1016/j.conengprac.2009.05.006.

[23] A. Sadeghian, J. Lavers, Dynamic reconstruction of nonlinear v-i characteristic in electric arc furnaces using adaptive neuro-fuzzy rule-based networks, Appl. Soft Comput. 11 (1) (2011) 1448–1456, https://doi.org/10.1016/j.asoc.2010.04.016.

[24] K.-L. Chang, S. Guillas, Computer model calibration with large non-stationary spatial outputs: application to the calibration of a climate model, J. R. Stat. Soc., Ser. C, Appl. Stat. 68 (1) (2018) 51–78, https://doi.org/10.1111/rssc.12309.

[25] S. Golestani, H. Samet, Generalised Cassie–Mayr electric arc furnace models, IET Gener. Transm. Distrib. 10 (13) (2016) 3364–3373, https://doi.org/10.1049/iet-gtd.2016.0405.

[26] J. Marulanda-Durango, A. Escobar-Mejía, A. Alzate-Gómez, M. Álvarez López, A support vector machine-based method for parameter estimation of an electric arc furnace model, Electr. Power Syst. Res. 196 (2021) 107228, https://doi.org/10.1016/j.epsr.2021.107228.

[27] D. Alkaran, M. Vatani, M. Sanjari, G. Gharehpetian, Parameters estimation of electric arc furnace based on an analytical solution of power balance equation, Int. Trans. Electr. Energy Syst. 27 (4) (2016) 1–11, https://doi.org/10.1002/etep.2295.

[28] S.M.M. Agah, S.H. Hosseinian, H.A. Abyaneh, N. Moaddabi, Parameter identification of arc furnace based on stochastic nature of arc length using two-step optimization technique, IEEE Trans. Power Deliv. 25 (4) (2010) 2859–2867.

[29] E. Acha, A. Semlyen, N. Rajakovic, A harmonic domain computational package for nonlinear problems and its application to electric arcs, IEEE Trans. Power Deliv. 5 (3) (1990) 1390–1397, https://doi.org/10.1109/61.57981.

[30] M. Torabian Esfahani, B. Vahidi, Development of optimal shunt hybrid compensator based on improving the measurement of various signals, Measurement 69 (2015) 250–263, https://doi.org/10.1016/j.measurement.2015.03.021.

[31] C.W. Cleghorn, B. Stapelberg, Particle swarm optimization: stability analysis using n-informers under arbitrary coefficient distributions, Swarm Evol. Comput. 71 (2022) 101060, https://doi.org/10.1016/j.swevo.2022.101060, https://www.sciencedirect.com/science/article/pii/S2210650222000323.

[32] A. Fathy, M.A. Elaziz, A.G. Alharbi, A novel approach based on hybrid vortex search algorithm and differential evolution for identifying the optimal parameters of PEM fuel cell, Renew. Energy 146 (2020) 1833–1845, https://doi.org/10.1016/j.renene.2019.08.046, https://www.sciencedirect.com/science/article/pii/S0960148119312339.

[33] B. Samieiyan, P. MohammadiNasab, M.A. Mollaei, F. Hajizadeh, M. Kangavari, Novel optimized crow search algorithm for feature selection, Expert Syst. Appl. 204 (2022) 117486, https://doi.org/10.1016/j.eswa.2022.117486, https://www.sciencedirect.com/science/article/pii/S0957417422008156.

[34] J. Tao, R. Zhang, Y. Zhu, DNA Computing Based Genetic Algorithm: Applications in Industrial Process Modeling and Control, Springer Nature, Singapore, 2020, https://books.google.com.co/books?id=6KR-zQEACAAJ.

[35] M. Talaat, Z. El-Shaarawy, M. Tayseer, A. El-Zein, An economic study concerning the cost reduction of the covered transmission conductors based on different optimization techniques, Results Eng. 11 (2021) 100262, https://doi.org/10.1016/j.rineng.2021.100262, https://www.sciencedirect.com/science/article/pii/S2590123021000633.

[36] R. Estran, A. Souchaud, D. Abitbol, Using a genetic algorithm to optimize an expert credit rating model, Expert Syst. Appl. 203 (2022) 117506, https://doi.org/10.1016/j.eswa.2022.117506.

[37] R. Hinterding, Gaussian mutation and self-adaption for numeric genetic algorithms, in: Proceedings of 1995 IEEE International Conference on Evolutionary Computation, vol. 1, 1995, pp. 384–386.

[38] D. Liu, Z. Hu, Q. Su, Neighborhood-based differential evolution algorithm with direction induced strategy for the large-scale combined heat and power economic dispatch problem, Inf. Sci. 613 (2022) 469–493, https://doi.org/10.1016/j.ins.2022.09.025.

[39] M. Klimas, D. Grabowski, Identification of nonstationary parameters of electric arc furnace model using Monte Carlo approach, in: 2020 Progress in Applied Electrical Engineering (PAEE), 2020, pp. 1–6.

[40] G. Galvan, S. Lucidi, A parameter-free unconstrained reformulation for nonsmooth problems with convex constraints, Comput. Optim. Appl. 80 (2021) 1–21, https://doi.org/10.1007/s10589-021-00296-1.

[41] O. Bozorg-Haddad, P. Sarzaeim, H.A. Loáiciga, Developing a novel parameter-free optimization framework for flood routing, Sci. Rep. 11.